Investigation of the Mechanism of Iron Release from the C-Lobe of Human Serum Transferrin: Mutational Analysis of the Role of a pH Sensitive Triad†

Peter J. Halbrooks,‡ Qing-Yu He,‡,§ Sara K. Briggs,‡ Stephen J. Everse,‡ Valerie C. Smith,|| Ross T. A. MacGillivray,|| and Anne B. Mason*,‡

Department of Biochemistry, University of Vermont, College of Medicine, 89 Beaumont Avenue, Burlington, Vermont 05405, and Department of Biochemistry and Molecular Biology, University of British Columbia, Vancouver, B.C. V6T 1Z3 Canada

Received October 28, 2002; Revised Manuscript Received January 17, 2003

ABSTRACT: The transferrins (TFs) are a family of proteins that are widely distributed in vertebrates, where they serve a major role in iron binding and transport. Most TFs are composed of two homologous lobes, the N- and C-lobes, each able to bind a single iron atom. Human serum transferrin (hTF) binds iron in the blood and delivers it to actively dividing cells; through the process of receptor-mediated endocytosis, diferric hTF in the serum (pH ∼7.4) binds to specific TF receptors on the cell surface and is internalized, whereupon a pH drop in the endosome (pH ∼5.6) facilitates iron release. Many factors affect the rate of iron release, including pH, chelator, temperature, salt, and lobe-lobe interactions. We, and others, have actively studied the mechanism of iron release from the recombinant N-lobe of hTF; in contrast, the exact details of iron release from the C-lobe have remained less well characterized but appear to differ from those found for the N-lobe. Recently, to simplify the purification protocol, we have expressed and purified full-length recombinant hTF containing an N-terminal hexahistidine tag [Mason et al. (2002) *Biochemistry 41,* 9448−9454]. In the present work, we have expressed a full-length recombinant hTF containing a K206E mutation such that the N-lobe does not readily release iron. The resulting full-length hTF allows us to focus on the C-lobe and to study the effects of mutations introduced into the C-lobe. The success of this strategy is documented and in vitro mutagenesis is used to identify three residues in the C-lobe that are critical for iron-release. Although the importance of this triad is unequivocally demonstrated, further studies are needed to completely elucidate the mechanism of iron release from the C-lobe of hTF. In addition, the striking difference in the effect of increasing salt concentrations on iron release from the two lobes of hTF is further documented in the present work.

Human serum transferrin (hTF)[1] is a member of the transferrin family of iron binding proteins. These proteins are characterized by an ability to bind two Fe (III) atoms reversibly; hTF is a glycoprotein made up of a 679 amino acid chain (∼80 kDa) arranged in two homologous lobes, termed the N- and C-lobes, each bearing a single iron-binding site. The two lobes share ∼40% sequence identity and are presumed to have arisen by a series of gene duplication and fusion events (*1*, *2*). Each lobe is further divided into two domains connected by two antiparallel β-strands which act as a hinge; in each lobe the iron binding site lies in this interdomain cleft (*3*, *4*).

Iron binding to and release from hTF occurs in a pH-dependent manner. Iron binds to the protein in the serum (pH ∼7.4) and is delivered to cells by receptor-mediated endocytosis. The diferric TF−receptor complex is targeted to an acidic endosome (pH ∼5.6) where the iron is released (*5*). The receptor and apo-TF return to the cell surface, and the apo-TF is released to pick up more iron and repeat the cycle. In vitro, the two lobes of hTF display different iron release properties (*6*−*8*). Iron release from the N-lobe is faster and occurs at a higher pH than release from the C-lobe.

The ability to produce recombinant hTF N-lobe (hTF/2N) efficiently has led to an extensive investigation of its iron release properties and development of a model for iron release (*9*). A pH dependent "dilysine trigger" plays a critical role in hTF/2N iron release. Protonation at low pH causes the two lysines (K206 and K296) to repel each other opening the cleft and releasing iron (*10*−*13*). In part, the different iron release properties of the C-lobe could stem from the absence of an equivalent pair of lysines. Dewan et al. (*14*) suggested that a triad comprised of K534, R632, and D634 might serve as the pH sensitive motif in the C-lobe. However,

† This work was supported by USPHS Grant R01 DK 21739 (ABM). This work was also supported by an award to the University of Vermont under the Howard Hughes Medical Institute Biomedical Research Support Program for Medical Schools

* To whom correspondence should be addressed. Telephone: (802) 656-0343 Fax: (802) 862-8229. E-mail: Anne.Mason@uvm.edu.

‡ University of Vermont.

§ Present address: Kadoorie Sciences Building, University of Hong Kong, Pokfulam, Hong Kong.

|| University of British Columbia.

[1] Abbreviations: TF, transferrin; hTF-Gly, commercially available glycosylated human serum transferrin; hTF-NG, recombinant nonglycosylated human serum transferrin; N-His hTF, comprised of the signal peptide followed by amino acids 1−4 from hTF, a hexa His-tag, a factor Xa cleavage site, and finally the coding region for amino acids 1−679 of hTF-NG; hTF/2N, the N-lobe of human serum transferrin; oTF/2N, the N-lobe of ovotransferrins; BHK cells, baby hamster kidney cells; Tiron, 4,5-dihydroxy-1,3-benzenedisulfonic acid; NTA, nitrilotriacetic acid; EDTA, ethylenediaminetetraacetate; oTF, ovotransferrins; LTF, lactoferrin; MES, morpholinoethanesulfonic acid; Hepes, *N*-(2-hydroxyethyl)piperazine-*N*′-ethanesulfonic acid.

10.1021/bi027071q CCC: $25.00
Published on Web 03/14/2003

work on the C-lobe has been hindered by an inability to produce sufficient protein by recombinant techniques to allow subsequent mutational analysis (*15*). A recent report by Zak and Aisen (*16*) suggests one solution to this problem. In the present report, we provide a second approach and demonstrate its utility and feasibility.

Through the introduction of a K206E mutation into the N-lobe of a full-length hTF, we have analyzed the independent kinetics of iron release from the C-lobe. To ensure homogeneity, the recombinant proteins are nonglycosylated (NG); for the purpose of purification, they contain a His tag at their amino terminus (N-His). Here, we show that N-His K206E hTF-NG serves as a good model for investigation of hTF C-lobe, as (1) the N-lobe does not readily release iron, leaving only the C-lobe to bind and release iron, and (2) the lobe-lobe interaction is preserved. At both pH 7.4 and pH 5.6, the iron release rate for the C-lobe is similar in hTF-NG with and without the K206E mutation. Scanning alanine mutagenesis of Dewan's putative pH-sensitive triad (*14*) shows that the loss of any one of these residues leads to an inability of the C-lobe to release iron at pH 7.4 under our standard conditions and a greatly reduced rate of iron release at pH 5.6. These results suggest that this trio of residues plays a role similar to the dilysine trigger and highlights the critical nature of these residues in the mechanism of iron release from the C-lobe.

MATERIALS AND METHODS

Construction of Plasmids with pNUT N-His K206E hTF-NG Containing K534A, R632A, D634A, and Q540A Mutations. The pNUT N-His K206E hTF-NG expression plasmid was constructed by ligating an *EcoRI-BamHI* DNA fragment from pNUT-hTF/2N K206E (*10*) with the *EcoRI-EcoRI* and *EcoRI*−*BamHI* fragments from hTF-NG (*17*). DNA fragments were purified using the Qiagen gel extraction kit and ligated in a triple ligation reaction. The correct fragment orientation was confirmed by restriction endonuclease mapping and DNA sequence analysis.

The C-lobe mutations (K534A, R632A, D634A, and Q540A) were introduced into the pNUT N-His K206E hTF-NG construct using the QuickChange mutagenesis kit (Stratagene). Two complimentary mutagenic oligonucleotide primers containing the mutations were used:

K534A
5′ AAG GGA GAT GTG GC**T** TTT GTG **GC**A CAC CAG ACT GTC CC 3′
5′ GGG ACA GTC TGG TGT **GC**C ACA AA**A** GCC ACA TCT CCC TT 3′
R632A
5′ GAA ACC AAG GAC CTT CTG TTC **GC**A GAT GAC ACA GTA TGT TTG GCC 3′
5′ GGC CAA ACA TAC TGT GTC ATC T**GC** GAA CAG AAG GTC CTT GGT TTC 3′
D634A
5′ GAA ACC AAG GAC CTT CTG TTC AGA GAT G**C**C ACA GTA TGT TT**A** GCC 3′
5′ GGC TAA ACA TAC TGT G**G**C ATC TCT GAA CAG AAG GTC CTT GGT TTC 3′
Q540A
5′ GTG AAA CAC CAG ACT GTC CC**G GC**G AAC ACT GG**A** GGA AAA AAC CC 3′
5′ GGG TTT TTT CCT CCA GTG TTC **GCC** GGG ACA GTC TGG TGT TTC AC 3′

The mutagenized nucleotides are shown in bold type. The conditions for the PCR reaction were as follows: initial denaturation at 95 °C for 30 s, followed by 18 cycles with denaturation at 95 °C for 30 s, annealing at 55 °C for 1 min, and extension at 68 °C for 15 min. To determine the presence of the correct mutation and absence of other mutations, the complete sequence of the transferrin cDNA and flanking pNUT sequences were determined prior to introduction of the plasmid into baby hamster kidney (BHK) cells.

Production and Purification of Recombinant Proteins. Recombinant hTF was expressed by BHK cells and purified from the tissue culture medium using procedures that have been described in detail elsewhere (*17, 18*). In short, the cell culture medium was concentrated and exchanged on a spiral concentrator followed by chromatography on a Poros 50 HQ column to remove phenol red and most of the serum albumin present in the media. The His tagged constructs were isolated by chromatography on a Qiagen Ni−NTA column using a BioCad Sprint chromatography system to simultaneously monitor the absorbance at 280 nm, the conductivity, and the pH. A Sephacryl S200HR column was used to eliminate imidazole and exchange the protein into 0.1 M NH_4HCO_3. The diferric hTF samples were then exchanged into 50 mM Hepes buffer (pH 7.4) using Centricon 30 microconcentrators and stored at −20 °C as concentrated stock solutions (∼2.5 mM).

Assay for Recombinant Protein. The amount of recombinant hTF in the tissue culture medium and at various stages of the purification was determined by an adaptation of a competitive solid-phase radioimmunoassay in which biotinylated hTF was substituted for iodinated sample as described previously (*18*).

Spectral Data. To assess iron binding for each recombinant hTF, UV−vis spectra were recorded on a Varian Cary 100 spectrophotometer (600 to 250 nm). Difference spectra were generated by subtracting the spectrum of Hepes buffer (50 mM, pH 7.4) from the sample spectra. The reported results are the average values derived from at least three such scans.

Kinetics of Iron Release. As described previously in detail (*17*), the kinetics of iron removal from transferrin at pH 7.4 were measured by monitoring the increase in absorbance at 480 nm for the release of iron to the chelator Tiron (4,5-dihydroxy-1,3-benzene-disulfonic acid, disodium salt monohydrate) using a dual-beam Cary 100 spectrophotometer. A thermostatable 6 × 6 multicell block peltier accessory allowed data collection on six samples at a time in the dual beam mode. Final concentrations of ∼6 μM of protein and 12 mM of Tiron in a total volume of 500 μL Hepes buffer (100 mM, pH 7.4) were used for these kinetic assays, and a circulating water bath maintained the temperature at 37 °C throughout the experiments. To ensure complete iron removal (which is essential for accurate determination of the rates), data were recorded until at least three half-lives had elapsed. The effect of salt on iron release was investigated by carrying out reactions at five concentrations of KCl up to 500 mM.

To measure the release of iron at pH 5.6, 50 mM MES was used as the reaction buffer, and 4 mM EDTA was used in place of Tiron. The buffer−chelator mixture was allowed to equilibrate prior to addition of the protein. Under the

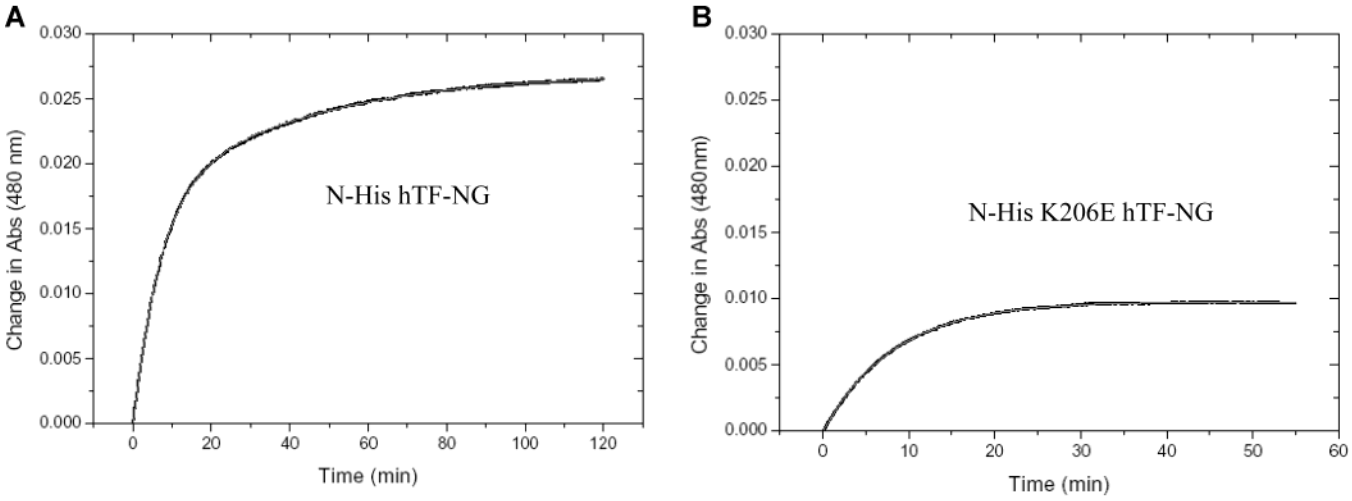

FIGURE 1: Kinetic curves reflecting the change in absorbance at 480 nm vs time at 37 °C, pH 7.4, 0.1 M Hepes, 12 mM Tiron, 0.3 M KCl, and 0.5 A_{280}/mL of protein. (A) Curve for iron-removal from N-His hTF-NG, best fit by two release rates, and (B) the curve for iron-removal from N-His K206E hTF-NG, best fit by a single release rate. Note that the time (*X*-axis) differs in the two panels.

conditions used, the release of iron from the protein was monitored directly by following the decrease in absorbance at the absorbance maximum of 293 nm. As reported previously (*17*), we found that the rate of iron release at pH 5.6 from the N-lobe was too fast to measure accurately using the Cary 100. Therefore, the rate of iron release from the N-lobe of N-His hTF-NG was determined using a stopped-flow technique on an OLIS RSM1000 spectrophotometer, again following the decrease in absorbance at the visible maximum (*19*). Iron release from the N-lobe was complete after two minutes. Therefore, the rate of release from the C-lobe of N-His hTF-NG at pH 5.6 was determined on the Cary 100 after discarding the first two minutes of data collection.

The curves resulting from a plot of absorbance versus time were fitted using the Origin Version 4.1 software (MicroCal, Inc). A single-exponential function best described the iron release rate from the N-His K206E hTF-NG mutant at pH 7.4; however, at pH 5.6, two release events were observed. To calculate the best fit to the resulting biphasic curve, the data from the first 40 min and the final 4000 minutes were fit independently; these time frames were attributed to iron release from the C-lobe and N-lobe, respectively. A double exponential function was required to fit the data derived from N-His hTF-NG at pH 7.4 and the double mutants at pH 5.6. In the latter cases, the amplitudes for two rate constants were averaged and fixed with the assumption that complete iron removal from each binding site contributes equally to the absorbance of the iron−Tiron complex (*17*). In all cases, excellent fits were obtained ($R^2 > 0.99$).

Iron Retention Level as a Function of pH. The retention of iron as a function of pH was measured for each mutant protein. Aliquots of iron-saturated protein were incubated in a buffer containing 33.3 mM Hepes, MES, and sodium acetate adjusted to the appropriate pH (between 3 and 8) with either 1 N NaOH or acetic acid. The protein solutions were maintained at 4 °C for a period of one week to allow each sample to reach equilibrium. The percentage of iron remaining bound to the TF samples was determined by measuring the absorbance at the visible absorption maxima and comparing this absorbance to that of the fully iron-loaded protein. The pH was measured on a blank set of tubes at the end of the experiment. The data were plotted and analyzed using Origin software.

RESULTS

To determine whether the rate of release of iron from the C-lobe of the N-His K206E hTF-NG construct is kinetically equivalent to the construct lacking the N-lobe mutation (N-His hTF-NG), the release rate as a function of salt concentration was determined for each at pH 7.4 and 37 °C. Kinetic curves for each of the two constructs at a single salt concentration of 0.3M KCl are shown in Figure 1. It must be remembered that at pH 7.4 the uptake of iron by the chelating agent Tiron is being monitored by tracking the increase in the absorbance at 480 nm, so the curve is positive, whereas at pH 5.6 with EDTA as chelator, the decrease in absorbance is followed. It was found that the curve for N-His hTF-NG was best fit by two rates (0.024 and 0.126 min^{-1} at 0.3M KCl) and that for N-His K206E hTF-NG by a single rate (0.125 min^{-1}). Note that the change in absorbance was approximately half for the N-His K206E hTF-NG construct versus the N-His hTF-NG construct, as would be expected if iron was being removed from a single site.

The rate of iron release for each construct (N-His K206E hTF-NG and N-His hTF-NG) was measured as a function of the salt concentration. The results of this experiment are presented in Figure 2. No iron was released from the N-lobe of N-His K206E hTF-NG at any of the KCl concentrations, as clearly indicated by the single rate obtained from the analysis and the half-maximal absorbance. In contrast, for the N-His hTF-NG construct, two rates were found over the full range of salt concentrations. Importantly, the results show that the C-lobe of N-His K206E hTF-NG releases iron at a rate that is identical to the C-lobe of N-His hTF-NG. This finding allows us to pursue C-lobe mutational studies with the assurance that no adverse effects on the function of the C-lobe are conferred by the K206E N-lobe mutation.

Having established that the N-His K206E hTF-NG is a suitable construct in which to place C-lobe mutations, we produced four mutant proteins in which either Lys 534, Arg

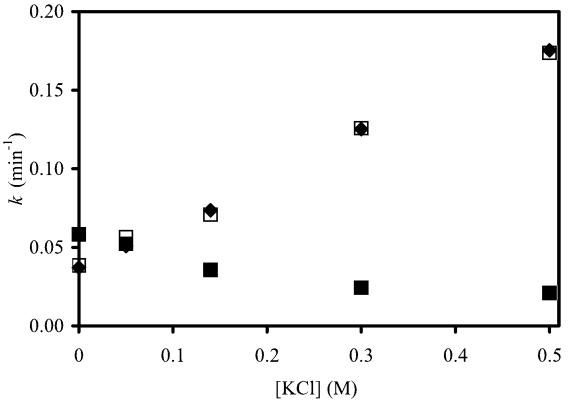

FIGURE 2: Observed rate constants for the removal of iron from each lobe of N-His hTF-NG and from the C-lobe of N-His K206E hTF-NG as a function of the KCl concentration. The rate constant as a function of KCl concentration was determined at 37 °C, pH 7.4, 0.1 M Hepes, 12 mM Tiron, and 0.5 A_{280}/mL of protein. Iron release for the N-lobe (■) and C-lobe (□) of N-His hTF-NG and the C-lobe of (◆) N-His K206E hTF-NG. (Note: No iron is released from the N-lobe of N-His K206E hTF-NG under the conditions used).

Table 1: Spectral Characteristics of Recombinant TF Species Used in This Study[a]

diferric protein	λ_{max} (nm)	λ_{min} (nm)	A_{max}/A_{min}	A_{280}/A_{max}
hTF-NG[b]	464	403	1.38	27.5
N-His hTF-NG[b]	466	403	1.13	21.3
N-His K206E hTF-NG	463	400	1.44	25.6
N-His K206E/**K534A** hTF-NG	467	405	1.39	25.3
N-His K206E/**R632A** hTF-NG	466	407	1.30	27.4
N-His K206E/**D634A** hTF-NG	463	405	1.30	27.5
N-His K206E/**Q540A** hTF-NG	463	401	1.46	23.0

[a] The four mutations in the C-lobe are shown in bold type. [b] From ref *17*.

632, Asp 634, or Gln 540 was substituted by alanine and placed into N-His K206E hTF-NG background. In each case, the amount of recombinant full-length His tagged protein produced and recovered was comparable to previous results obtained for the N-His tagged hTF-NG constructs (*17*, *18*). To confirm that the recombinant proteins were able to bind iron in each lobe, UV/vis scans were performed and intrinsic spectral parameters (λ_{max}, λ_{min}, A_{max}/A_{min}, and A_{280}/A_{max}) were measured. The results are presented in Table 1. The λ_{max} and λ_{min} for each of the iron-loaded double mutants are virtually identical to those found for both N-His hTF-NG and hTF-NG. The spectral data indicate that each mutant is loaded with iron in both lobes and that none of the mutations has a measurable effect on the geometry of the iron-binding sites.

The release rate of iron from three of the mutant hTFs was determined at both pH 7.4 and 5.6 at a constant temperature of 37 °C (Table 2A,B). The particular pHs were chosen because of their physiological relevance to the pH of the serum (∼7.4) and the putative pH of the endosome (∼5.6). As reported above, the rate of release of iron at pH 7.4 from the C-lobe is equivalent whether the K206E mutation in the N-lobe is absent or present ($k = 0.040$ min^{-1} for the nonmutated protein and 0.037 min^{-1} for the K206E mutant). This appears to be true at pH 5.6 as well, ($k =$ 0.127 vs 0.139 min^{-1}). Significantly, at pH 7.4, there is little or no release of iron from either the N-lobe or the C-lobe for any of the three mutants under the conditions used to release iron from the nonmutated C-lobe (Table 2A). At pH 5.6 and 37 °C, the rate of iron release from the N-lobe of the N-His K206E hTF-NG mutant ($k = 0.0006$ min^{-1}) relative to N-lobe lacking the K206E mutation ($k = 2.610$ min^{-1}) is slowed ∼4400-fold. In addition, the rate of iron release for each of the residues of the C-lobe triad at pH 5.6 and 37 °C, is extremely slow. The constructs containing the R632A and D634A mutations yield similar rates of release, while the K534A mutant releases iron at a marginally faster rate (Table 2B). All three of the C-lobe mutants release iron at rates that are slightly faster than the rate measured for the N-lobe containing the K206E mutation. In all cases, it was necessary to collect data over a period of almost 3 days to allow complete release of iron from both lobes (greater than 3 half-lives).

The effect of pH on iron release was also determined by an equilibrium approach. It is important to note that no chelator is present in these samples. Thus, over the period of 1 week, a slow protonation of the iron binding residues leads to release at acidic pH even in the absence of a chelator (*20*). Obviously, because iron is being released from each lobe of each protein we are measuring an average for both. To obtain a rough estimate of the pH at which half of the iron was released, the curves were fit to a sigmoidal function. The results of this analysis are presented in Table 3. The pH at which 50% of the iron was released for the two commercial glycosylated hTFs, (Boehringer Mannheim and Intergen) and for the recombinant nonglycosylated hTF with and without an N-terminal His tag was within experimental error. The pH at which 50% of the iron was released for the mutants containing the K206E mutation and for the three C-lobe mutants was downshifted slightly. The poorer fit of the release data for the K534A and R632A mutants (indicated by the larger value for χ^2) suggests the presence of two species in these particular samples. The data are more descriptive than quantitative but provide an independent assessment of binding stability under equilibrium conditions.

DISCUSSION

Our previous studies established that the presence of a hexa-His tag at the N-terminus of hTF-NG had no effect on the rate of iron release from either lobe when compared to hTF-NG lacking a His tag (*17*). This finding provided a basis for pursuing the present work using the His tagged construct; both ease of production and purification are critical to the success in studies aimed at assessing the mechanism of iron release from the C-lobe. To concentrate efforts on the C-lobe and to simplify the interpretation of the results, the next logical step was to produce a recombinant hTF in which the ability of the N-lobe to release iron was largely curtailed. As described in the introduction, extensive work (*10*−*13*) had established the significant role of a pair of lysines (K206 and K296) in the release of iron from the N-lobe. Crystal structures of hTF/2N (*21*) and oTF/2N (*14*) indicate that these lysine residues (which reside in different domains) share a hydrogen bond when the two domains come together as a result of iron binding. Our studies with the isolated N-lobe indicated that the K206E mutation effectively "locks" the N-lobe into a closed conformation at pH 7.4 and greatly reduces the rate of iron release at pH 5.6. These previous studies showed that the two opposing lysines serve as an

Table 2: Iron Release Rates at the Conditions Shown

diferric protein	k_N (min^{-1}) × 10^{-3}	k_C (min^{-1}) × 10^{-3}	n^a	time (min)	ratio (k_N/k_C)
(A) pH 7.4,100 mM Hepes Buffer, 12 mM Tiron as Chelator @ 37 °C					
N-His hTF-NG	54.7 ± 3.3	40.4 ± 1.3	3	120	1.4
N-His K206E hTF-NG	no release	37.0 ± 1.7	3	120	–
N-His K206E/**K534A** hTF-NG	no release	no release	4		–
N-His K206E/**R632A** hTF-NG	no release	no release	4		–
N-His K206E/**D634A** hTF-NG	no release	no release	4		–
(B) pH 5.6,50 mM MES Buffer, 4 mM EDTA as Chelator @ 37 °C					
N-His hTF-NG	2610.0 ± 33.4[b]	126.9 ± 5.6	4	40	20.6
N-His K206E hTF-NG	0.60 ± 0.02	139.1 ± 6.0	4	4000	4400
N-His K206E/**K534A** hTF-NG	0.57 ± 0.04	5.2 ± 0.05	4	4000	0.11
N-His K206E/**R632A** hTF-NG	0.60 ± 0.05	1.5 ± 0.09	4	4000	0.41
N-His K206E/**D634A** hTF-NG	0.44 ± 0.07	1.1 ± 0.09	3	4200	0.41
(C) pH 7.4,100 mM Hepes Buffer, 12 mM Tiron as Chelator @ 25 °C					
N-His hTF-NG[c]	22.7 ± 0.9	6.4 ± 0.6	4	400	3.5
N-His K206E/**Q540A** hTF-NG	no release	34.9 ± 0.8	3	170	

[a] Number of independent measurements made. [b] Determined using stopped flow on the OLIS RSM1000. [c] From ref *17*.

Table 3: Iron Release as a Function of pH in the Absence of Chelator[a]

protein	source	χ^2	pH at which 50% iron released	comment
Fe_2hTF-Gly	Boehringer Mannheim	19.3	4.55 ± 0.05	
Fe_2hTF-Gly	Intergen	9.9	4.56 ± 0.04	
Fe_2hTF-NG	recombinant	18.0	4.56 ± 0.08	
Fe_2N-His hTF-NG	recombinant	2.9	4.59 ± 0.02	
Fe_2N-His K206E hTF-NG	recombinant	4.9	4.21 ± 0.02	
Fe_2N-His K206E/**K534A** hTF-NG	recombinant	25.0	4.19 ± 0.06	2 species?
Fe_2N-His K206E/**R632A** hTF-NG	recombinant	22.0	4.11 ± 0.17	2 species?
Fe_2N-His K206E/**D634A** hTF-NG	recombinant	7.4	4.36 ± 0.04	

[a] The data were fit using the Boltzman equation for a sigmoidal curve (Origin). C-Lobe mutations are shown in bold type.

active trigger that helps open the N-lobe, rather than a "lock" whose disabling would passively allow the lobe to open. This point is perhaps best illustrated by the fact that neither the K206A nor the K296A N-lobe mutants readily release iron (*11*). In the present study, we introduced the K206E mutation into the full-length N-His tagged construct. Our previously reported release rate for the N-lobe K206E mutant at pH 7.4 (6.42 ± 0.04 (min^{-1}) × 10^{-5}) was based on an extrapolation from a 5-h assay in which only about 2% of the iron was removed (*10*). We now realize that such extrapolations are not justifiable, and in the present work, we clearly show that it is impossible to measure a rate of iron release from the N-lobe of the N-His K206E hTF-NG construct under our standard conditions at pH 7.4. Kinetic analysis at both pH 7.4 and 5.6 clearly indicates that the presence of the K206E mutation in our recombinant hTFs effectively disables iron release from the N-lobe, while the rate of iron release from the C-lobe is unaffected (Figure 2 and Table 2A,B). This allows determination of iron-release from the C-lobe in the context of a full-length, bilobal molecule. It also indicates that the release rate of iron from the C-lobe is completely unaffected by whether the N-lobe is open or closed implying a lack of cooperatively between the lobes under our conditions.

Direct comparison of the experimental rates measured at pH 7.4 and 5.6 is precluded by the use of different buffers and chelators. Unfortunately we, and others, have been unable to identify conditions that allow direct comparisons at these two pHs. Therefore, legitimate comparisons can only be made within each group, with the release rate of iron from the N- and C-lobes of N-His hTF-NG providing an internal control.

The results shown in Figure 2 also confirm the previously observed differential effect of salt on the iron release behavior of the two lobes at pH 7.4 (*22*, *23*). Increasing KCl affects the release rates from the two lobes in an opposite manner. There is a nearly linear increase in the rate of iron release from the C-lobe as a function of salt concentration. Conversely, increasing salt concentrations leads to a nonlinear decrease in the rate of iron release from the N-lobe, as previously described for the recombinant N-lobe at neutral pH (*9*). This striking difference in the effect of salt on the rate of release of iron from the two lobes of hTF indicates a fundamental difference in the mechanism by which iron is released from each lobe. In addition, our previous studies were carried out at 25 °C (*17*), yielding a ratio (k_N/k_C) of 3.5 for N-His hTF-NG (Table 2C). As shown in Table 2A at pH 7.4 and 37 °C, there is a 2.4-fold increase in the release rate from the N-lobe and a nearly 6-fold increase in the rate of release from the C-lobe resulting in a ratio (k_N/k_C) of 1.4. Thus, the iron release rate from the C-lobe is more sensitive to both salt and temperature than the release rate from the N-lobe.

The identification of a triad of residues equivalent to the dilysine trigger by Dewan et al (*14*) was based on examination of the hTF structure (3.3 Å) determined by Zuccola (*24*). In this structure, the OD2 of the carboxylate group of Asp 634 is 3.4 Å from the Lys 534 NZ and 3.3 Å from the NH2 group of Arg 632. Dewan suggested that lowering the pH would result in weakening or breaking of the hydrogen bonds bridging the Arg and Lys residues. More recently, higher-resolution crystal structures of both porcine and rabbit serum transferrins have become available (*25*). Examination of the porcine structure (2.15 Å) (Figure 3A) confirms that the three

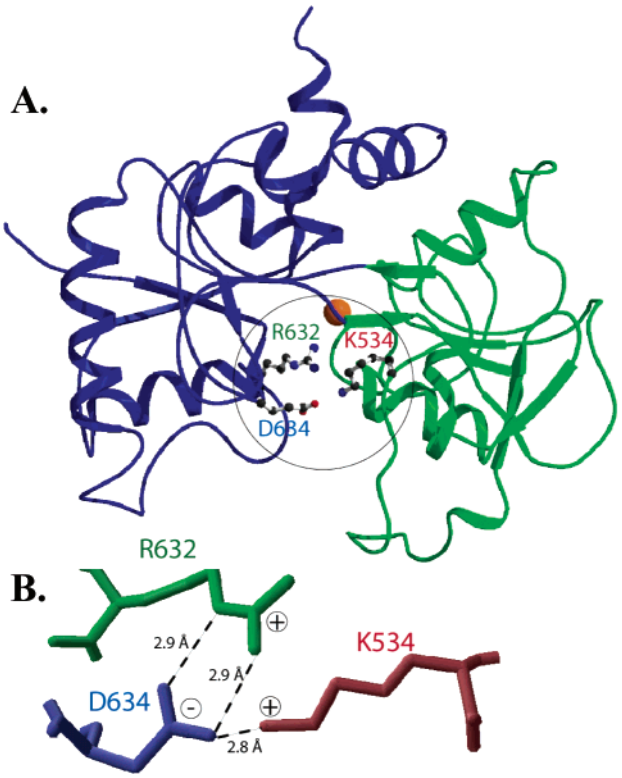

FIGURE 3: Ribbon diagram of the C-lobe of porcine serum transferrin (*25*). (A) The residues of the triad are shown in the iron bound state using human serum transferrin numbering. (B) Close-up view of the triad with potential hydrogen bonds shown. This figure was prepared using Bobscript (*30*, *31*) and Raster3D (*32*, *33*).

residues, Lys 543, Arg 641, and Asp 643 (equivalent to Lys 534, Arg 632, and Asp 634 in hTF), are linked to each other in a hydrogen-bonding network (Figure 3B) and shows that the distances between these residues are <3 Å. The Lys 534 residue resides in the CII domain and is equivalent to Lys 206 in the N-lobe. The Arg 632 residue resides in the CI domain and is equivalent to Lys 296. The bridging residue, Asp 634, is also located in the CI domain. Given the hypothesis that the negatively charged Asp 634 in hTF stabilizes the positive charges of the Lys and Arg residues, we anticipated that the D634A mutation would de-stabilize the triad and lead to a faster rate of iron release from the C-lobe. This is definitely not the case, since release of iron from the D634A mutant differs only slightly from the other two mutants. In a manner highly reminiscent of the dilysine trigger in the N-lobe, the triad appears to serve as a trigger that helps to initiate iron release rather than as a lock that prevents it. Each residue of this triad must play an active role in the process of iron-release from the C-lobe, since mutation of any of these residues to an alanine drastically slows chelator-mediated iron-release.

Examination of the pig structure also showed that Gln 549 (Gln 540 in the human structure) was in hydrogen bonding distance to both the Lys and Asp residues of the triad, raising the possibility that a tetrad of amino acids controls iron release in the C-lobe. To test this possibility, we expressed and purified a mutant in which this Gln residue at position 540 was mutated to alanine. As shown in Table 2C, the C-lobe of the Q540A mutant released iron at a 5−6-fold faster rate than that found for the control protein at 25 °C and pH 7.4. We conclude that the Gln residue at position 540 is not directly involved in the mechanism of iron release from the C-lobe defined by the Asp−Arg−Lys triad.

Table 4: Sequence Alignment of TFs Family Members Highlighting Residues of the Dilysine Trigger (K206 and K296) and the Proposed Triad (K534, R632, and D634) in Various Species[a]

	N-lobe		C-lobe		
residue #	206[b]	296	534	632	634
human TF	K	K	K	R	D
rabbit TF	K	K	K	R	D
rat TF	K	K	K	R	D
murine TF	K	K	K	R	D
horse TF	K	K	K	R	D
porcine TF	K	K	K	R	D
bovine TF	K	K	K	R	D
melanoTF	K	K	***R***	***K***	***A***
human LTF	***R***	K	K	***N***	***N***
chicken oTF	K	K	***Q***	***K***	***L***

[a] Numbering is based on hTF sequence; nonconserved residues are shown in bold type and are italicized. The alignments are made with BLOSUM 62 score tables with default settings and displayed using GeneDoc (*29*). [b] Note 206 in the N-lobe is equivalent to 534 in the C-lobe and 296 is equivalent to 632.

It is interesting, and perhaps significant, that both Lys 296 and Arg 632 are immediately preceded by a reverse γ turn (comprised of the sequence of Leu-Leu-Phe) which is found in all mammalian TFs, as well as in LTF and oTF. Also potentially significant is the observation that Arg 632 and Lys 534 are each directed toward the center of one of the liganding tyrosine residues. In fact, both the dilysine trigger (in the N-lobe) and the Lys−Arg−Asp triad (in the C-lobe) are surrounded by a "box" of tyrosine residues homologous in both lobes. This hydrophobic box has been suggested as a mechanism to reduce the pK_as of the Arg and Lys and to facilitate deprotonation (*12*, *14*, *26*).

The importance of the triad in the C-lobe is highlighted by comparison of the amino acid sequence of TFs from different species including the rabbit and pig, as shown in Table 4. Each member of the triad is completely conserved in all the mammalian serum TFs but not in other family members (melanotransferrin, human LTF or chicken oTF), implying fundamental differences in the details of iron release for C-lobes of these other proteins.

An alternate hypothesis to identifying the C-lobe triad as the critical pH dependent stabilizing/destabilizing structural feature controlling iron release from the C-lobe is that the triad participates in the mechanism of chelator-dependent iron removal. The presence of a kinetically significant anion binding (KISAB) site(s) in the C-lobe has been proposed (*27*, *28*). Presumably such a site(s) serves as a target for binding of an anion and/or chelator leading to release of iron. Work by the Aisen lab previously identified Lys 569 as a possible KISAB site(*23*). The K569Q mutant featured a 15−20-fold reduction in the rate of iron release from the C-lobe at pH 5.6 compared to nonmutated C-lobe. We find differences of 26-, 88-, and 121-fold for the K534A mutant, the R632A mutant, and the D634A mutant, respectively (Table 2B). Collectively these results indicate that more than one KISAB site probably exists. Further work is needed to determine the effect of salt on the release rate of each mutant to determine whether like the dilysine pair in the N-lobe, the Lys, and Arg residues also function as anion binding sites.

In summary, the K206E mutation introduced into N-His hTF-NG disables iron release from the N-lobe at pH 7.4 and drastically slows it at pH 5.6. Iron release from the C-lobe is unaffected at both pH 7.4 and 5.6, thus allowing an investigation of release properties of the C-lobe in the context of full-length hTF. We have introduced four different C-lobe point mutations into N-His K206E hTF-NG with the aim of investigating the mechanism of iron release from the C-lobe. The choice of three of these mutations was based on a report by Dewan et al. (*14*). Indeed, under our standard conditions, when any of the three residues is converted to an alanine, iron release is completely inhibited at pH 7.4 and extremely slowed at pH 5.6, confirming the importance of this triad. Equilibrium data qualitatively support the results from the kinetic experiments. We conclude that disruption of the dilysine trigger in the N-lobe and of the triad in the C-lobe result in the inability to release iron from either lobe within a physiologically relevant time frame.

REFERENCES

1. Williams, J. (1982) The evolution of transferrin, *TIBS 7*, 394−397.
2. Yang, F., Lum, J. B., McGill, J. R., Moore, C. M., Naylor, S. L., van Bragt, P. H., Baldwin, W. D., and Bowman, B. H. (1984) Human transferrin: cDNA characterization and chromosomal localization, *Proc. Natl. Acad. Sci. U.S.A. 81*, 2752−2756.
3. Evans, R. W., Crawley, J. B., Joannou, C. L., and Sharma, N. D. (1999) Iron Proteins, in *Iron and Infection: Molecular, Physiological and Clinical Aspects* (Bullen, J. J., and Griffiths, E., Eds.) pp 27−86, John Wiley and Sons, Chichester, U.K.
4. Aisen, P., Enns, C., and Wessling-Resnick, M. (2001)Chemistry and biology of eukaryotic iron metabolism, *Int. J. Biochem. Cell Biol. 33*, 940−959.
5. Klausner, R. D., Ashwell, G., van Renswoude, J., Harford, J. B., and Bridges, K. R. (1983)Binding of apotransferrin to K562 cells: explanation of the transferrin cycle, *Proc. Natl. Acad. Sci. U.S.A. 80*, 2263−2266.
6. Princiotto, J. V., and Zapolski, E. J. (1975) Difference between the two iron-binding sites of transferrin, *J. Biol. Chem. 253*, 1930−1937.
7. Lestas, A. N. (1976) The effect of pH upon human transferrin: selective labeling of the two iron-binding sites, *Br. J. Haematol. 32*, 341−350.
8. Baldwin, D. A., De Sousa, D. M. R., and Von Wandruszka, R. M. A. (1982) The Effect of pH on the Kinetics of Iron Release from Human Transferrin, *Biochim. Biophys. Acta 719*, 140−146.
9. He, Q.-Y., and Mason, A. B. (2002) Molecular aspects of release of iron from transferrins, in *Molecular and Cellular Iron Transport* (Templeton, D. M., Ed.) pp 95−123, Marcel Dekker, Inc., New York.
10. He, Q.-Y., Mason, A. B., Tam, B. M., MacGillivray, R. T. A., and Woodworth, R. C. (1999) Dual role of Lys206-Lys296 interaction in human transferrin N-lobe: Iron-release trigger and anion-binding site, *Biochemistry 38*, 9704−9711.
11. Nurizzo, D., Baker, H. M., He, Q.-Y., MacGillivray, R. T. A., Mason, A. B., Woodworth, R. C., and Baker, E. N. (2001) Crystal structures and iron release properties of mutants (K206A and K296A) that abolish the dilysine interaction in the N-lobe of human transferrin, *Biochemistry 40*, 1616−1623.
12. Steinlein, L. M., Ligman, C. M., Kessler, S., and Ikeda, R. A. (1998) Iron release is reduced by mutations of lysine 206 and 296 in recombinant N-terminal half-transferrin, *Biochemistry 37*, 13696−13703.
13. Li, Y. J., Harris, W. R., Maxwell, A., MacGillivray, R. T. A., and Brown, T. (1998) Kinetic studies on the removal of iron and aluminum from recombinant and site-directed mutant N-lobe half transferrins, *Biochemistry 37*, 14157−14166.
14. Dewan, J. C., Mikami, B., Hirose, M., and Sacchettini, J. C. (1993) Structural evidence for a pH-sensitive dilysine trigger in the hen ovotransferrin N-lobe: Implications for transferrin iron release, *Biochemistry 32*, 11963−11968.
15. Mason, A. B., Tam, B. M., Woodworth, R. C., Oliver, R. W. A., Green, B. N., Lin, L.-N., Brandts, J. F., Savage, K. J., Lineback, J. A., and MacGillivray, R. T. A. (1997) Receptor recognition sites reside in both lobes of human serum transferrin, *Biochem. J. 326*, 77−85.
16. Zak, O., and Aisen, P. (2002) A new method for obtaining human transferrin C-lobe in the native conformation: preparation and properties, *Biochemistry 41*, 1647−1653.
17. Mason, A. B., He, Q. Y., Halbrooks, P. J., Everse, S. J., Gumerov, D. R., Kaltashov, I. A., Smith, V. C., Hewitt, J., and MacGillivray, R. T. A. (2002) Differential effect of a His tag at the N- and C-termini: Functional studies with recombinant human serum transferrin, *Biochemistry 41*, 9448−9454.
18. Mason, A. B., He, Q.-Y., Adams, T. E., Gumerov, D. R., Kaltashov, I. A., Nguyen, V., and MacGillivray, R. T. A. (2001) Expression, Purification, and Characterization of Recombinant Nonglycosylated Human Serum Transferrin Containing a C-Terminal Hexahistidine Tag, *Protein Expression Purif. 23*, 142−150.
19. He, Q. Y., Mason, A. B., Nguyen, V., MacGillivray, R. T. A., and Woodworth, R. C. (2000) The chloride effect is related to anion binding in determining the rate of iron release from the human transferrin N-lobe, *Biochem. J. 350*, 909−915.
20. Abdallah, F. B., and Chahine, J. M. E. (2000) Transferrins: Iron release from lactoferrin, *J. Mol. Biol. 303*, 255−266.
21. MacGillivray, R. T. A., Moore, S. A., Chen, J., Anderson, B. F., Baker, H., Luo, Y. G., Bewley, M., Smith, C. A., Murphy, M. E., Wang, Y., Mason, A. B., Woodworth, R. C., Brayer, G. D., and Baker, E. N. (1998) Two high-resolution crystal structures of the recombinant N-lobe of human transferrin reveal a structural change implicated in iron release, *Biochemistry 37*, 7919−7928.
22. Egan, T. J., Ross, D. C., Purves, L. R., and Adams, P. A. (1992) Mechanism of Iron Release from Human Serum C−Terminal Monoferric Transferrin to Pyrophosphate: Kinetic Discrimination Between Alternative Mechanisms, *Inorg. Chem. 31*, 1994−1998.
23. Zak, O., Tam, B., MacGillivray, R. T. A., and Aisen, P. (1997) A kinetically active site in the C-lobe of human transferrin, *Biochemistry 36*, 11036−11043.
24. Zuccola, H. J. (1993) *The Crystal Structure of Monoferric Human Serum Transferrin*, Dissertation, Georgia Institute of Technology, Atlanta.
25. Hall, D. R., Hadden, J. M., Leonard, G. A., Bailey, S., Neu, M., Winn, M., and Lindley, P. F. (2002) The crystal and molecular structures of diferric porcine and rabbit serum transferrins at resolutions of 2.15 and 2.60 A, respectively, *Acta Crystallogr.., Sect. D 58*, 70−80.
26. Clarkson, J., and Smith, D. A. (2001) UV Raman evidence of a tyrosine in apo-human serum transferrin with a low pK_a that is elevated upon binding of sulphate, *FEBS Lett. 503*, 30−34.
27. Marques, H. M., Watson, D. L., and Egan, T. J. (1991) Kinetics of Iron Removal from Human Serum Monoferric Transferrins by Citrate, *Inorg. Chem. 30*, 3758−3762.
28. Marques, H. M., Walton, T., and Egan, T. J. (1995) Release of iron from C-terminal monoferric transferrin to phosphate and pyrophosphate at pH 5.5 proceeds through two pathways, *J. Inorg. Biochem. 57*, 11−21.
29. Nicholas, K. B., Nicholas, H. B., and Deerfield, D. W. I. (1997) GeneDoc: Analysis and Visualization of Genetic Variation, *EMBNEW NEWS 4*, 14.
30. Esnouf, R. M. (1997) An extensively modified version of Molscript which includes greatly enhanced coloring capabilities, *J. Mol. Graphics 15*, 133−138.
31. Kraulis, P. (1991) Molscript; A program to produce both detailed and schematic plots of protein structures, *J. Appl. Crystallogr. 24*, 946−950.
32. Bacon, D. J., and Anderson, W. F. (1988) A fast algorithm for rendering − filling molecular pictures, *J. Mol. Graphics 6*, 219−220.
33. Merritt, E. A., and Murphy, M. E. P. (1994) Raster3D, version 2.0: A program for photorealistic molecular graphics, *Acta Crystallogr., Sect. D 50*, 869−873.

BI027071Q